Desalination and Water Treatment
www.deswater.com

doi: 10.5004/dwt.2017.0490

62 (2017) 57–65
February

Porous polyethersulfone hollow fiber membrane in oily wastewater treatment

Gh. Bakeri*, Z. Fallahnejad

Membrane Research Lab, Faculty of Chemical Engineering, Babol Noshirvani University of Technology, Babol, Iran, Tel. +98 912 526 5739; Fax: +98 11 323 34 204; emails: bakeri@nit.ac.ir (G. Bakeri), Zeynab_fallahnejad@yahoo.com (Z. Fallahnejad)

Received 2 May 2016; Accepted 12 July 2016

ABSTRACT

Oily wastewater from oil refineries and oil distribution centers is one of the most important environmental concerns in recent decades; therefore, it is critical to treat these types of wastewaters. In this study, the performance of three different polyethersulfone hollow fiber membranes in synthetic oily wastewater treatment has been investigated, and the effects of operating conditions such as transmembrane pressure, oil concentration in the feed and feed cross flow velocity (CFV) on the membrane performance were studied. Increasing the pressure makes more membrane compactness and higher membrane fouling; therefore, higher pressure reduces the membrane performance. The optimum operating conditions for oily wastewaters separation are: P = 1 bar, low feed concentration (300 ppm) and high feed CFV (0.18 m s^{-1}). In this study, membrane #M1 with the mean pore size of 8.29 nm, membrane porosity of 77%, permeation flux of 12.4 (L m^{-2} hr^{-1}) and 100% oil rejection presented the best performance in treating synthetic oily wastewaters.

Keywords: Synthetic oily wastewater; Polyethersulfone (PES) hollow fiber membrane; Environmental pollution; Membrane cleaning

1. Introduction

Due to the impact of oily wastewaters on the environment, the wastewaters from oil refineries and oil distribution centers should be treated before discharging to sewage [1]. Depending on the geographical conditions and characteristics of oily wastewater, there are varieties of standards in different countries, e.g., in Malaysia the maximum limit is 10 ppm while in the United States of America, it is 40 ppm [2]. The traditional methods for treatment of oily wastewater such as gravity separation and skimming, dissolved air flotation, de-emulsification, coagulation and flocculation are not effective in removing the oil droplets and emulsions. These methods have several disadvantages such as low efficiency, high operating costs, corrosion and recontamination of treated stream. Furthermore, these processes are effective when the size of oil droplet in the oil-in-water emulsion is between 20 and 150 μm. All of these disadvantages promoted the development of new processes for treatment of oily wastewaters especially when the size of oil droplet is small [3].

Different kinds of membrane-based processes such as ultrafiltration (UF), nanofiltration (NF) and reverse osmosis (RO) have been effectively used for oil/water separation. Membrane-based filtration processes are playing a major role in oily wastewater separation, due to their advantages such as no need to chemical additives to break the emulsion, high chemical oxygen demand (COD) removal efficiency and smaller equipments [1]. Because of its suitable pore size and its capability in removing emulsified oil droplets without any de-emulsification processes and, furthermore, low operating pressure, which reduces the energy consumption, UF process has been verified as an efficient method for treatment of oil-in-water emulsions [4]. Pressure-driven UF process is widely used for separation, purification and concentration of dispersed materials in liquids.

A number of researches have been focused on the application of UF and microfiltration (MF) membranes

* Corresponding author.

in oily wastewater, where oil droplets are retained by the membrane and the continuous phase permeates [5–10]. Lipp et al. reported that since the oil droplets are deformable and depending on the applied pressure, the oil droplets can be squeezed through the pores and contaminate the permeate [11]. Nazzal and Wiesner found that if the transmembrane pressure (TMP) is below the critical value, the oil rejection could be maximized [12]. Hlavacek reported that the porous structure of membrane could promote coalescence of micron-size and submicron-size oil droplets into larger ones that can easily be separated by gravity. In this study, the membrane acts as a coalescer rather than as a separator [13]. Mueller et al. investigated the application of ceramic and polymeric MF membranes in treating synthetic oil-in-water emulsion, containing 250–1,000 ppm heavy crude oil with a diameter of 1–10 μm, and reported that the membranes produce water with oil content less than 6 ppm [14]. Kong and Li investigated the effects of feed flow rate, operating pressure, membrane pore size and porosity on the separation of oil-in-water emulsions by flat sheet hydrophobic polyvinylidene fluoride (PVDF) membranes [15].

Most of the researches on the application of polyethersulfone (PES) membrane in synthetic oily wastewater have been devoted to flat sheet membranes. The objective of this study is the application of PES hollow fiber membranes in synthetic oily wastewater and investigation on the effect of operating parameters such as TMP, feed concentration and feed cross flow velocity (CFV) on the performance of membranes. The membrane performance is characterized in terms of pure water flux (PWF), permeate flux (PF) and percentage of oil rejection (%R).

2. Experimental setup

2.1. Preparation of spinning solutions

PES was purchased from Arkema Inc. (USA) and was dried at 70°C overnight before dissolution in solvent. N-Methyl-2-pyrrolidone (NMP; CAS No. 872-50-4) with a purity of 99.5 wt% was purchased from Merck (Germany) and was used as solvent without further purification. A predetermined amount of PES was dissolved in NMP at 70°C under gentle mixing to make the PES solution with desired concentration. The compositions of the spinning solutions are presented in Table 1.

2.2. Preparation of hollow fiber membrane

Dry jet-wet spinning technique was used for fabrication of the membranes. The spinning solution was delivered to the annulus of a tube-in-orifice spinneret at constant flow rate while water as the bore fluid was sent to the inner tube of the spinneret. After leaving the spinneret and passing through the air gap, the nascent fiber entered the coagulation bath (tap water) to complete the phase inversion process. The wet spun fibers were immersed in water for several days to remove the residual solvent and then dried naturally by hanging vertically at room temperature. The spinning conditions are listed in Table 2.

Table 1
The compositions of the polymer solutions

Solution No.	PES (wt%)	Solvent (wt%)	Solution viscosity (centipoise)
#M1	17	83	285.6
#M2	19	81	505.5
#M3	21	79	802.1

2.3. Materials

Commercial grade gas oil from NIORDC (Iran), dish-washing detergent and deionized water (with a conductivity of 2.9 μS cm^{-1}) were used for making the oil-in-water emulsion. The detergent was used to make the oil-in-water emulsion with higher stability. Ethylenediaminetetraaceticacid (EDTA) and sodium dodecyl sulfate (SDS) were used for preparation of the solution for membrane cleaning.

2.4. Membrane characterization

Asymmetric porous membranes were characterized in terms of membrane porosity and mean pore size where the membrane porosity (ε) was defined as the volume of the pores divided by the total volume of the porous membrane. The method for determination of membrane porosity, which is related to the membrane structure, was reported elsewhere [16]. Pure water permeation test was used for determination of membrane mean pore size [17].

Furthermore, the contact angle of water with the membrane surface is a criterion for surface hydrophilicity that affects on the permeance and fouling characteristics of membrane, and is measured by the sessile drop technique using contact angle goniometer (model G1, Krüss GmbH, Hamburg, Germany). At least ten points on the surface of membrane were used for contact angle measurement, and the results were averaged.

To measure the membrane porosity, some hollow fibers were immersed for a few days in methanol and water, respectively, to completely wet the membranes. Then, the weight of wet membranes was measured by a balance. Afterward, the free water on the surface of fibers was removed by a tissue, and the water in the lumen side of the fibers was discharged through blowing air for a short period of time. Then, the fibers were dried at 45°C for 12 h, and the weight of dried membranes was measured. The membrane porosity was calculated by using Eq. (1):

$$\varepsilon = \frac{\frac{w_1 - w_2}{\rho_w}}{\frac{w_1 - w_2}{\rho_w} + \frac{w_2}{\rho_p}} \quad (1)$$

Table 2
Hollow fiber spinning conditions

Air gap (cm)	1
External coagulant	Water
Bore fluid temperature	Room temperature
External coagulant temperature	Room temperature

where w_1 is the weight of wet membrane (g); w_2 is the weight of dry membrane (g); ϱ_p is the density of the polymer (1.55 g cm^{-3} for PES) and ϱ_w is the density of water (1 g cm^{-3}).

The mean pore size of membrane (r_m), which is a representative of pore size along the membrane thickness, was measured by pure water permeation test. Pure water, with a pressure of 1 bar, was sent to the shell side of membrane module, and the flow rate of water, permeated through the lumen side of the fibers, was measured. The mean pore size of the membrane was calculated through Eq. (2) (Guerout–Elford–Ferry equation):

$$r_m = \sqrt{\frac{8\eta l Q(2.9-1.75\varepsilon)}{\varepsilon A \Delta P}} \quad (2)$$

where η is the water viscosity (8.9 × 10^{-4} Pa s); l is the membrane thickness (m); ΔP is the operating pressure (0.1 MPa); Q is the flow rate of the permeated water (m^3 s^{-1}) and A is the effective area of the membrane (m^2).

2.5. Preparation of oil-in-water emulsion

Gas oil, dishwashing detergent and deionized water were mixed severely by mechanical stirrer (rpm = 2,500) for 5 min to make a stable oil-in-water emulsion. The concentration of oil was changed in the UF experiments (300, 600 and 900 ppm) whereas the concentration of detergent was constant (100 ppm).

2.6. Cross flow UF experiments

The schematic of the UF system and the membrane module are shown in Fig. 1 where the prepared oil-in-water emulsion as the feed solution is sent to the shell side of the UF module and the permeate is collected via the lumen side. The feed flow rate is controlled by the valve at the exit of the liquid. The permeation flux (J) and oil rejection (R) are calculated through Eqs. (3) and (4):

$$J = \frac{Q}{At} \quad (3)$$

$$R = (1 - \frac{C_P}{C_F}) \times 100 \quad (4)$$

where Q is the volume of the permeate (m^3); A is the effective area of the membrane (m^2); t is the time for collection of permeate (s); C_p is the concentration of the oil in the permeate and C_F is the concentration of the oil in the feed.

The range of operating conditions for UF experiments are summarized in Table 3 for each membrane.

During the experiments, no separation of oil from water was observed in the feed solution; in other words, the feed solutions were stable. The concentration of gas oil in water was analyzed by UV-VIS spectrophotometer (model: ChromTech) at 200 nm.

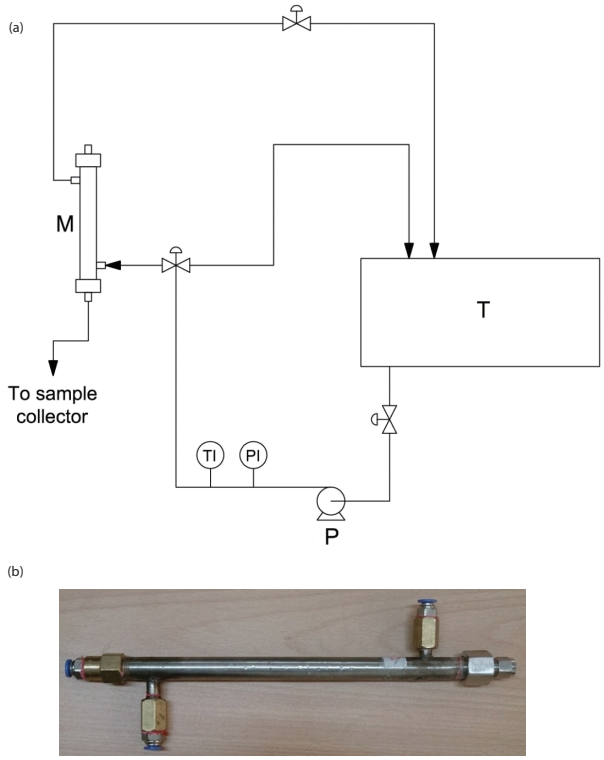

Fig. 1. (a) Schematic of cross flow ultrafiltration system: M = membrane module, T = feed tank, P = pump, PI = pressure indicator, and TI = temperature indicator, and (b) membrane module.

Table 3
The range of operating conditions in UF experiments

Membrane	Gas oil concentration (ppm)	Pressure (bar)	Temperature (°C)
M1	300, 600, 900	1, 2, 3	27
M2	300, 600, 900	1, 2, 3	27
M3	300, 600, 900	1	27

2.7. Cleaning of the fouled hollow fiber membranes

Due to the membrane fouling, the permeation flux decreases with time during the filtration process. The membrane cleaning procedure was obtained experimentally and was carried out between each run through the following steps:

Step 1: Washing the membranes by the cleaning solution (EDTA + SDS + water) at 45°C for 20 min. The cleaning solution enters to the shell side of the membrane module and exits from the lumen side.
Step 2: Washing the membranes by pure water at 50°C for 30 min.
Step 3: Washing the membranes in reverse direction (backwashing) by the cleaning solution (EDTA + SDS + water) at 45°C for 30 min.
Step 4: Backwashing the membranes by pure water at 50°C for 30 min.

The temperature of the cleaning solutions was increased to enhance the cleaning performance.

Table 4
The characteristics tests results of the fabricated PES hollow fiber membranes

Membrane No.	Water contact angle	Mean pore radius (nm)	Membrane porosity (%)	Inner diameter (mm)	Outer diameter (mm)
M1	77.13 ± 1.28	8.29	77	0.55	0.75
M2	82.17 ± 1.98	7.43	75	0.5	0.75
M3	83.16 ± 1.96	6.70	71	0.5	0.80

2.8. Scanning electron microscopy (SEM) test

SEM was used to observe the structure of membrane cross section. The fiber was broken in liquid nitrogen to make a smooth surface and then platinum (Pt) sputtered. The micrographs were taken by SEM (TM 3000, Hitachi (Japan)) with magnifications of 500 (cross section) and 5,000 (surface).

3. Results and discussion

3.1. Membrane characteristics

The characteristics tests results of the fabricated membranes are presented in Table 4 where increasing the polymer concentration in the spinning solution decreases the mean pore size of the membrane that is a rational conclusion. Furthermore, the porosity of the fabricated membranes reduced by increasing the polymer concentration. In addition, the contact angle of the membrane with water increases with polymer concentration; it should be mentioned that the contact angle of the membrane depends on different surface properties of membrane such as pore size and pore size distribution, surface roughness, surface hydrophobicity etc.; the smaller the pore size, the higher the contact angle.

The SEM micrographs of the outer surface and cross section for the fabricated membranes are presented in Fig. 2 where all membranes show skin layers on both inner and outer surfaces and fingerlike macrovoids, originating from inner and outer surfaces and extending to the middle of membrane cross section. This structure is related to the low viscosity of polymer solution and strong internal and external coagulants (water) that accelerate the phase inversion process [18].

3.2. The effect of operating pressure on the permeation flux

The plots of permeation flux (in terms of L m^{-2} hr^{-1}) vs. CFV at different pressures for membrane #M1 are presented in Fig. 3 where increasing the pressure enhances the flux but the flux decreases with increasing the concentration of the oil in the feed. Similar trends were observed for the other two membranes. The higher oil concentration makes more resistance for water to pass through the membrane and reduces the permeation flux while higher pressure provides more driving force and improves the permeation rate.

The flux increases with the pressure as it is the driving force in UF process but the increase is not exactly linear that can be related to the additional transfer resistances such as adsorption of oil droplets on the surface of the membrane and the effect of concentration polarization [19].

On the other hand, membrane fouling increases with the operating pressure. Higher pressure increases the compactness of oil layer on the surface of the membrane, which enhances the fouling of membrane. Furthermore, at higher pressure, the oil droplets are pushed into the membrane pores, which promotes the fouling. Therefore, increasing the pressure has negative effect on the permeation flux. In Fig. 4, the pressure normalized permeation fluxes of membrane #M2 (in terms of L m^{-2} h^{-1} bar^{-1}) are plotted vs. CFV at different feed concentration, which shows the decline in flux as the pressure increases that can be related to concentration polarization effect and pore blockage [20]. The same trends were observed for the other two membranes. Furthermore, the permeation flux of membrane #M1 is the highest that can be related to the higher porosity and bigger mean pore size of this membrane.

At higher pressure, there is more collision between emulsified oil droplets, which in turn breaks the film between the oil droplet and water, causing oil droplets to coalesce and form larger droplets. A layer containing large oil droplets starts to form just above the membrane surface, which, in turn, may be compressed on the membrane surface at higher pressure and leading to more membrane fouling [10]. This phenomenon reduces the flux.

The permeation flux vs. time for the fabricated membranes is presented in Fig. 5 where the permeation flux is leveled off for all the membranes after a specific time that is related to stabilization of the fouling process. The total membrane resistance consists of two main parts: pore blockage and concentration polarization. In the early stages of the filtration process, oil droplets precipitate in the pores of membrane and cause the decrease in the permeation flux. After stabilization the pore blockage phenomenon, the concentration polarization, which is related to the settling of the oil droplets on the surface of membrane, has the major role in the flux reduction [21]. It is interesting that the bigger the pore size of the membrane, the higher the pore blockage effect.

3.3. Effect of feed CFV on the permeation flux

The effect of feed CFV on the permeation flux of the fabricated membranes is shown in Fig. 6 where the flux increases with CFV that is related to the higher turbulency on the surface of the membrane (the Reynolds number increases from 100 to 2,200), which reduces the precipitation of the oil droplets on the surface of the membrane and, furthermore, decreases the effect of concentration polarization.

3.4. The effect of operating conditions on the gas oil rejection

Generally, membrane with bigger pore size has lower separation performance in the synthetic oily wastewater separation process. The oil rejection of the fabricated membranes

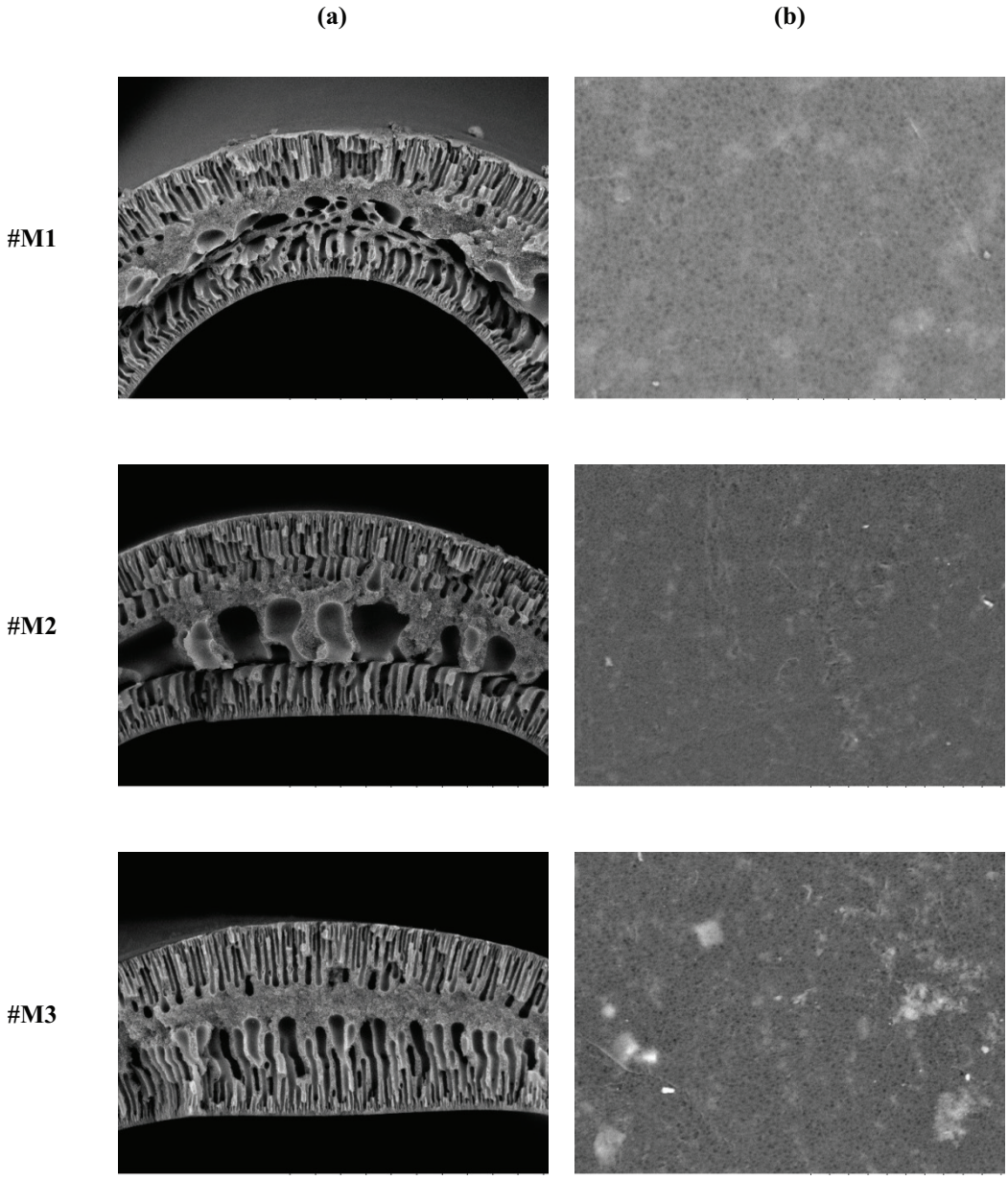

Fig. 2. SEM micrographs of the fabricated membranes: (a) cross section and (b) outer surface.

at the optimum pressure (P = 1 bar), oil concentration of 900 ppm and at different feed cross flow velocities are presented in Table 5. The same trends were observed at oil concentration of 300 and 600 ppm. Increasing the feed CFV enhances the mass transfer coefficient in the concentration boundary layer on the membrane surface and may decrease the rejection. All of the fabricated membranes show complete separation of oil from water that is related to the smaller membrane pore size compared with the size of the oil droplets. Furthermore, the skin layers on the inner and outer surfaces of membrane reduce the transport of the oil droplets through the membrane pores and enhance the oil rejection.

Based on the European standards, the maximum oil content in the treated oily wastewater is 5 ppm [22]; therefore, the fabricated PES membranes are suitable candidates for treatment of synthetic oily wastewater.

The reduction in permeation flux and enhancement in the oil rejection with increasing the oil concentration in the feed is a rational conclusion due to the effect of concentration polarization and formation of the oil cake on the membrane surface, which acts as a barrier for the permeation and as a pre-filter for the oil separation; these phenomena were reported in other studies. Furthermore, since the oil droplets are not rigid (deformable), they can be deformed at higher pressure and enter the membrane's pores, reducing the oil rejection even though the flux increases. In this study, the oil rejection is 100% at all investigated operating conditions because of the small pore size of the fabricated membranes.

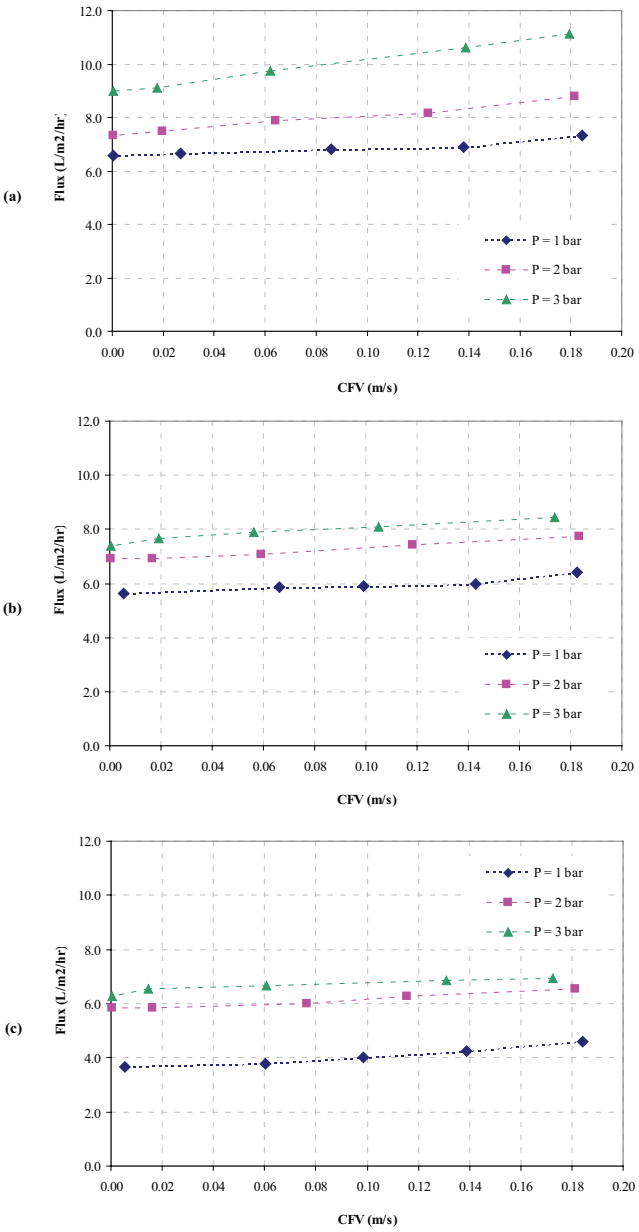

Fig. 3. The effect of operating pressure on the permeation flux of membrane #M1; oil concentration in the feed: (a) 300 ppm, (b) 600 ppm, and (c) 900 ppm.

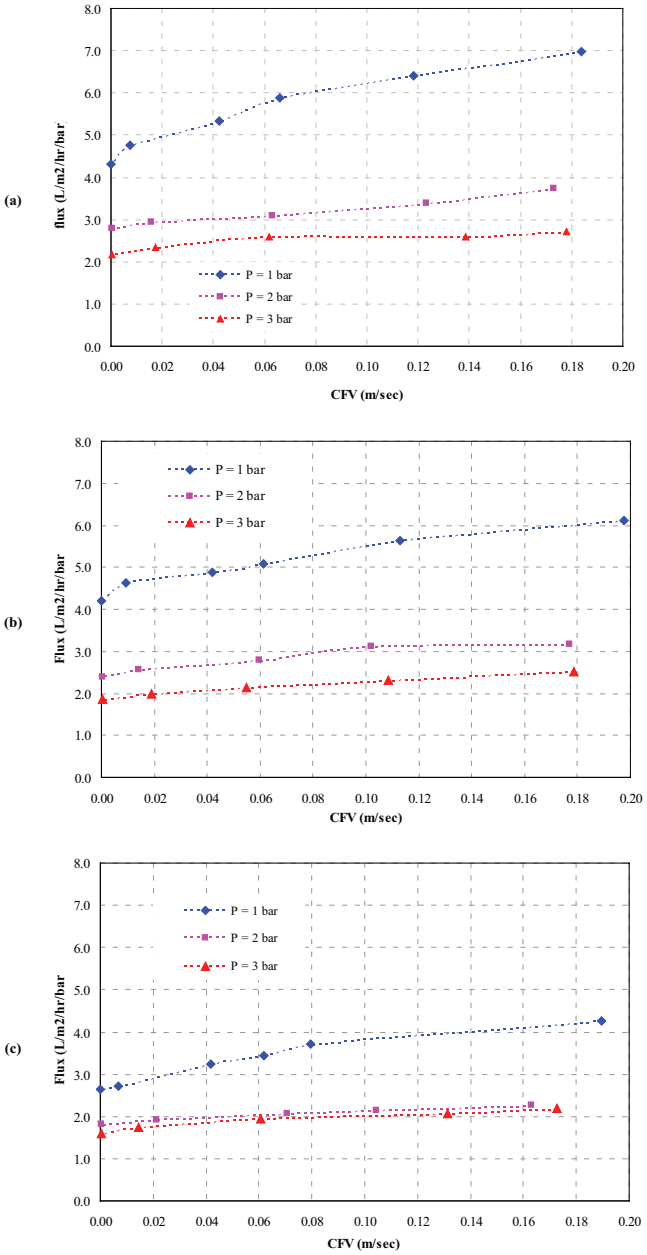

Fig. 4. The effect of operating pressure on the normalized permeation flux of membrane #M2 (in terms of L m^{-2} h^{-1} bar^{-1}); oil concentration in the feed: (a) 300 ppm, (b) 600 ppm, and (c) 900 ppm.

3.5. The flux recovery of hollow fiber membranes after membrane cleaning

After each UF experiment, the membrane was cleaned, and the flux recovery of the membrane is calculated through Eq. (5):

$$\text{Flux recovery (\%)} = \frac{J_f}{J_w} \times 100 \tag{5}$$

where J_f is the water permeation flux of membrane after cleaning (L m^{-2} h^{-1}), and J_w is the water permeation flux of fresh membrane (L m^{-2} h^{-1}). The flux recovery of the fabricated membranes at different operating conditions is shown in Fig. 7 where the smaller the membrane pore size or the higher the operating pressure of UF experiment, the less the flux recovery. Smaller membrane pore size promotes the irreversible fouling of the membrane and reduces the recovery. Furthermore, higher operating pressure during UF experiment may push the oil droplets into the pores and making irreversible fouling in the pore or on the surface of the membrane [23].

3.6. The membrane fouling analysis

The long-term performance of the fabricated membranes in terms of permeation flux is shown in Fig. 8 where the

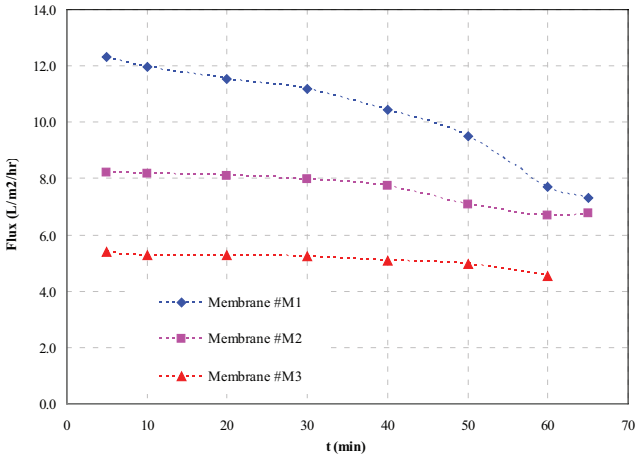

Fig. 5. Variation of permeation flux (in terms of L m^{-2} h^{-1}) with time for the fabricated membranes; feed oil concentration: 300 ppm, P = 1 bar, CFV = 0.18 m s^{-1}.

membranes showed stable operation after rapid decline in the flux during the initial 100 min operation.

The decline in the permeation flux is related to the fouling phenomenon during operation that is attributed to the adsorption of oil droplets in the pores of membrane, the concentration polarization effect and the accumulation of oil droplets on the surface of the membrane. Furthermore, the membrane has an intrinsic resistance against the permeation that is related to the structure of the membrane and is measured through pure water permeation test, as shown in Eq. (6):

$$R_m = \frac{\Delta P}{\mu J_{wf}} \tag{6}$$

where R_m is the intrinsic resistance of the membrane (m^{-1}); ΔP is the TMP (Pa); J_{wf} is the water permeation flux of fresh membrane (m^3 m^{-2} s^{-1}) and μ is the viscosity of the permeate (that is the water viscosity, 8.9 x 10^{-4} Pa.s) [24]. Furthermore, the resistances related to the concentration polarization phenomenon (R_{cp}), cake formation on the surface of membrane (R_c) and the adsorption of oil particles (R_a) can be measured through the procedure described elsewhere [6,25–27]. After long-term UF experiment, the membranes were flushed with water for 10 min, and then, the pure water permeation rate was measured (J_c). After that, the membrane was cleaned chemically for 10 min, and then, the pure water permeation flux was measured (J_a). The resistances were calculated through Eqs. (7)–(9):

$$R_{cp} = \frac{\Delta P}{\mu J_a} - R_m \tag{7}$$

$$R_c = \frac{\Delta P}{\mu J_c} - R_m - R_{cp} \tag{8}$$

$$R_a = \frac{\Delta P}{\mu J_{cp}} - R_m - R_{cp} - R_c \tag{9}$$

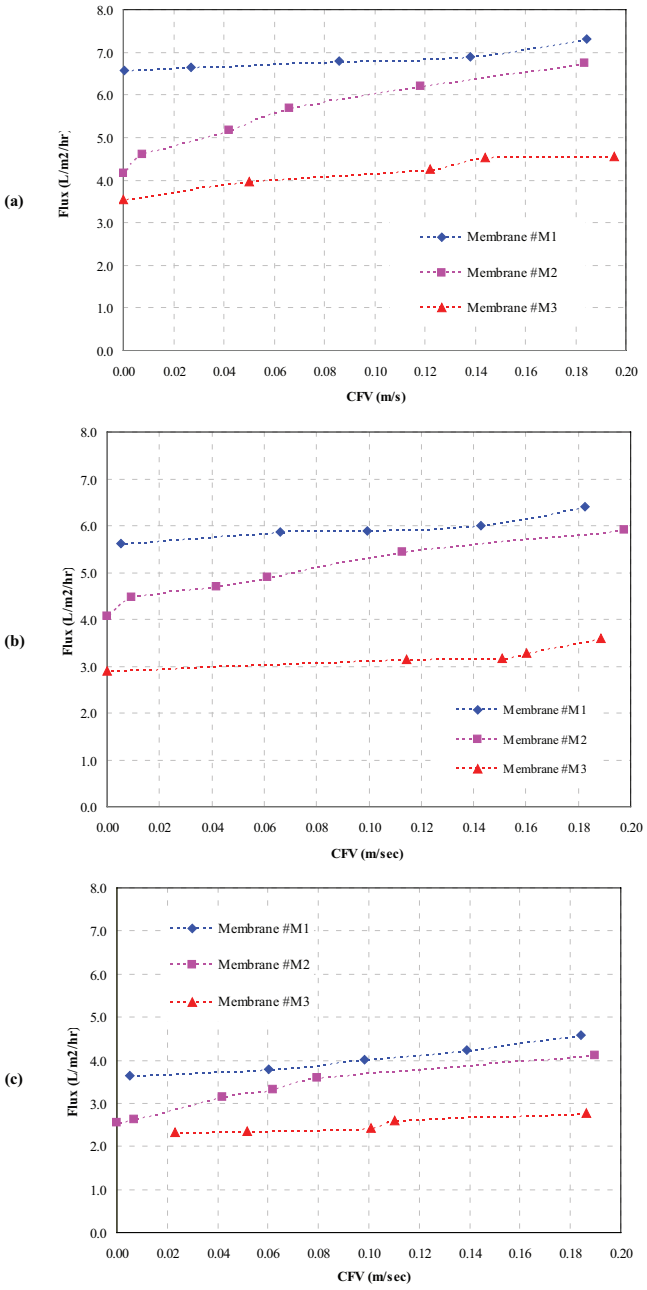

Fig. 6. The effect of feed cross flow velocity (CFV) on the permeation flux (PF) (in terms of L m^{-2} h^{-1}); P = 1 bar, gas oil concentration: (a) 300 ppm, (b) 600 ppm, and (c) 900 ppm.

where J_{cp} is the permeation flux of the membrane at the end of UF experiment. The calculated resistances are presented in Fig. 9 where the smaller the membrane pore size, the higher the intrinsic resistance of the membrane. Deformation of oil droplets, coagulation of oil droplets and making larger one and compaction affect on the resistance of cake layer. Furthermore, due to the entrance of oil droplets into the membrane pores, cake layer forms on the surface of the pore walls. After stabilization of the pore blockage phenomenon, the concentration polarization is created on the membrane surface [28,29].

Table 5
The oil rejection of PES membranes at different feed cross flow velocity (CFV); P = 1 bar, oil concentration in the feed: 900 ppm

Membrane #M1		Membrane #M2		Membrane #M3	
CFV (m/s)	Rejection (%)	CFV (m/s)	Rejection (%)	CFV (m/s)	Rejection (%)
0.18	100	0.19	100	0.19	100
0.14	100	0.08	100	0.11	100
0.10	100	0.06	100	0.10	100
0.06	100	0.04	100	0.05	100
0.01	100	0.01	100	0.02	100

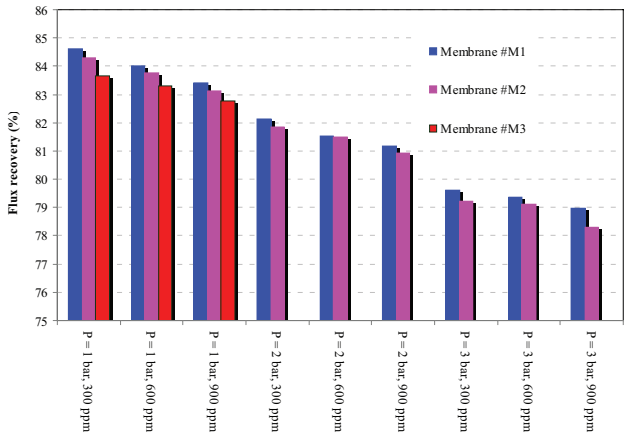

Fig. 7. The flux recovery of the fabricated membranes at different operating conditions.

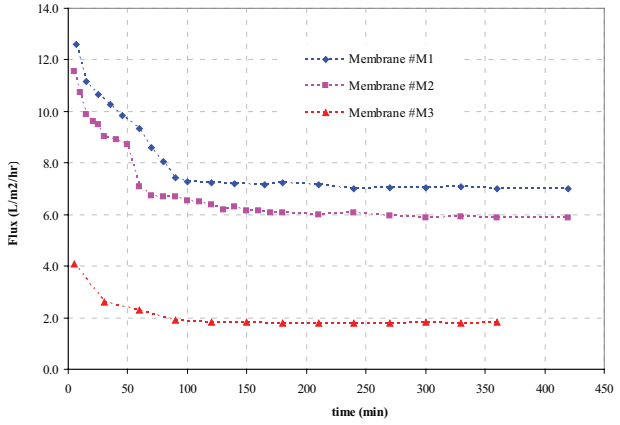

Fig. 8. The plot of permeation flux of the fabricated membrane vs. time, P = 1 bar, oil concentration in feed = 300 ppm.

4. Conclusions

In this study, the treatment of oily wastewaters by PES hollow fiber membranes through a cross flow UF system was investigated. The effects of membrane pore size on the permeation flux, oil rejection and flux recovery have been investigated. Furthermore, the effects of TMP, feed CFV and feed concentration on the membrane performance were studied.

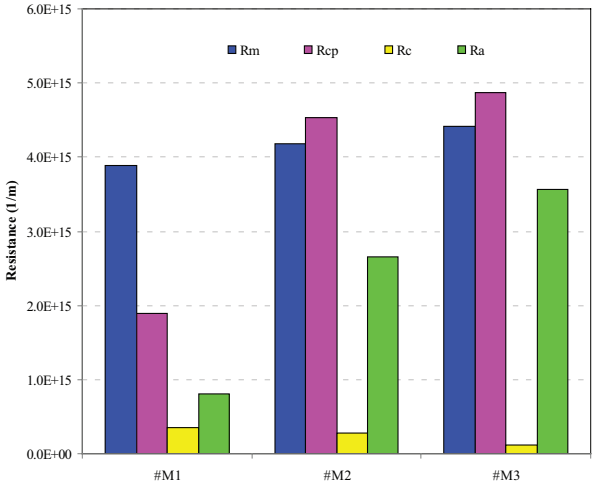

Fig. 9. The various resistances for the fabricated membranes: R_m = intrinsic resistance, R_{cp} = concentration polarization resistance, R_c = cake layer resistance, and R_a = adsorption resistance.

The conclusions are as follows:

- The permeation flux increases with the TMP but due to the existence of other resistances such as adsorption of oil on the membrane surface and the concentration polarization effect, the flux doesn't increase linearly with pressure. Considering the flux, oil rejection and membrane fouling, the optimum TMP is 1 bar.
- The membrane porosity, mean pore size and the structure of the membrane sublayer have major role on the permeation flux, flux deterioration and membrane fouling. The flux of membrane #M1 is the highest that can be related to the higher porosity and larger mean pore size of this membrane.
- Permeation flux decreases with the oil concentration in the feed and increases with CFV that the latter one is related to the higher turbulency on the surface of the membrane, which reduces the precipitation of oil droplets on the surface of membrane and, furthermore, decreases the effect of concentration polarization. In this study, all of the PES hollow fiber membranes effectively separate the oil from water.
- Membrane with bigger pore size shows higher flux recovery after membrane cleaning that is related to less irreversible fouling in the membrane pores or on the surface of the membrane.

References

[1] Y.S. Li, L. Yan, C.B. Xiang, L.J. Hong, Treatment of oily wastewater by organic-inorganic composite tubular ultrafiltration (UF) membranes, Desalination, 196 (2006) 76–83.

[2] C.S. Ong, W.J. Lau, P.S. Goh, B.C. Ng, T. Matsuura, A.F. Ismail, Effect of PVP molecular weights on the properties of PVDF-TiO_2 composite membrane for oily wastewater treatment process, Sep. Sci. Technol., 49 (2014) 2303–2314.

[3] L. Yan, S. Hong, M.L. Li, Y.S. Li, Application of the Al_2O_3-PVDF nanocomposite tubular ultrafiltration (UF) membrane for oily wastewater treatment and its antifouling research, Sep. Purif. Technol., 66 (2009) 347–352.

[4] W. Chen, J. Peng, Y. Su, L. Zheng, L. Wang, Z. Jiang, Separation of oil/water emulsion using Pluronic F127 modified polyethersulfone ultrafiltration membranes, Sep. Purif. Technol., 66 (2009) 591–597.

[5] B. Chakrabarty, A.K. Ghoshal, M.K. Purkait, Ultrafiltration of stable oil-in-water emulsion by polysulfone (PSF) membrane, J. Membr. Sci., 325 (2008) 427–437.

[6] J. Zhou, D. Wandera, S.M. Husson, Mechanisms and control of fouling during ultrafiltration of high strength wastewater without pretreatment, J. Membr. Sci., 488 (2015) 103–110.

[7] X. Huang, W. Wang, Y. Liu, H. Wang, Z. Zhang, W. Fan, L. Li, Treatment of oily waste water by PVP grafted PVDF ultrafiltration membranes, Chem. Eng. J., 273 (2015) 421–429.

[8] A. Salahi, T. Mohammadi, R. Mosayebi Behbahani, M. Hemmati, Asymmetric polyethersulfone ultrafiltration membranes for oily wastewater treatment: synthesis, characterization, ANFIS modeling, and performance, J. Environ. Chem. Eng., 3 (2015) 170–178.

[9] S. Jamaly, A. Giwa, S.W. Hasan, Recent improvements in oily wastewater treatment: progress, challenges, and future opportunities, J. Environ. Sci., 37 (2015) 15–30.

[10] M. Padaki, R. Surya Murali, M.S. Abdullah, N. Misdan, A. Moslehyani, M.A. Kassim, N. Hilal, A.F. Ismail, Membrane technology enhancement in oil–water separation - a review, Desalination, 357 (2015) 197–207.

[11] P. Lipp, C.H. Lee, A.G. Fane, C.J.D. Fell, A fundamental study of the ultrafiltration of oil-water emulsions, J. Membr. Sci., 36 (1988) 161–177.

[12] F.F. Nazzal, M.R. Wiesner, Microfiltration of oil-in-water emulsion, Water Environ. Res., 68 (1996) 1187–1191.

[13] M. Hlavacek, Break up of oil-in-water emulsions induced by permeation through a microfiltration membrane, J. Membr. Sci., 102 (1995) 1–7.

[14] J. Mueller, Y. Cen, R.H. Davis, Crossflow microfiltration of oily water, J. Membr. Sci., 129 (1997) 221–235.

[15] J. Kong, K. Li, Oil removal from oil-in-water emulsions using PVDF membranes, Sep. Purif. Technol., 16 (1999) 83–93.

[16] E. Yuliwati, A.F. Ismail, T. Matsuura, M.A. Kassim, M.S. Abdullah, Effect of modified PVDF hollow fiber submerged ultrafiltration membrane for refinery oily wastewater, Desalination, 283 (2011) 214–220.

[17] E. Yuliwati, A.F. Ismail, Effect of additives concentration on the surface properties and performance of PVDF ultrafiltration membranes for refinery produced wastewater treatment, Desalination, 273 (2011) 226–234.

[18] Gh. Bakeri, T. Matsuura, A.F. Ismail, The effect of phase inversion promoters on the structure and performance of polyetherimide hollow fiber membrane using in gas-liquid contacting process, J. Membr. Sci., 383 (2011) 159–169.

[19] H. Ohya, J.J. Kim, A. Chinen, M. Aihara, S.I. Semenova, Y. Negishi, O. Mori, M. Yasuda, Effects of pore size on separation mechanisms of microfiltration of oily water, using porous glass tubular membrane, J. Membr. Sci. 145 (1998) 1-14.

[20] A.B. Koltuniewicz, R.W. Field, Process factors during removal of oil-in-water emulsions with cross-flow microfiltration, Desalination, 105 (1996) 79–89.

[21] C. Zhao, J. Xue, F. Ran, S. Sun, Modification of polyethersulfone membranes, a review of methods, Prog. Mater Sci., 58 (2013) 76–150.

[22] R.V. Lopez, S. Elmaleh, N. Ghaffor, Cross-flow ultrafiltration of hydrocarbon emulsions, J. Membr. Sci., 102 (1995) 55–64.

[23] S. Hong, R.S. Faibish, M. Elimelech, Kinetics of permeate flux decline in crossflow membrane filtration of colloidal suspensions, J. Colloid Interface Sci., 196 (1997) 267–277.

[24] I.S. Chang, S.O. Bag, C.H. Lee, Effects of membrane fouling on soluble rejection during membrane filtration of activated sludge, Process Biochem., 36 (2001) 855–860.

[25] H. Shan, Membrane Fouling during the Microfiltration of Primary and Secondary Wastewater Treatment Plant Effluents Master Thesis, University of Pittsburgh, Master's Thesis, 2004.

[26] B. Eychene, C. Guigui, C. Cabassud, Engineering of an MBR supernatant fouling layer by fine particles addition: a possible way to control cake compressibility, Water Res., 45 (2011) 2060–2072.

[27] N.A.A. Hamid, A.F. Ismail, T. Matsuura, A.W. Zularisam, W.J. Lau, E. Yuliwati, M.S. Abdullah, Morphological and separation performance study of polysulfone/titanium dioxide (PSF/TiO_2) ultrafiltration membranes for humic acid removal, Desalination, 273 (2011) 85–92.

[28] L. Fan, J.L. Harris, F.A. Roddick, N.A. Booker, Influence of the characteristics of natural organic matter on the fouling of microfiltration membranes, Water Research 35 (2001) 4455–4463.

[29] E.H. Bouhabila, R.B. Aim, H. Buisson, Fouling characterization in membrane bioreactors, Separation and Purification Technology 22-23 (2001) 123–132.